PERGAMON

European Journal of Cancer 39 (2003) 728–735

European Journal of Cancer

www.ejconline.com

Review

Potential role of magnetic resonance spectroscopy in assessment of tumour response in childhood cancer

S.J. Vaidya[a], Geoffrey S. Payne[b], Martin O. Leach[b], C.R. Pinkerton[a,*]

[a]*Department of Paediatric Oncology, Institute of Cancer Research and The Royal Marsden NHS Trust, Sutton, Surrey SM2 5PT, UK*
[b]*Cancer Research UK Clinical Magnetic Resonance Research Group, Institute of Cancer Research and The Royal Marsden NHS Trust, Sutton, Surrey SM2 5PT, UK*

Received 29 April 2002; received in revised form 25 October 2002; accepted 8 November 2002

Abstract

This brief review considers to what extent Magnetic Resonance Spectroscopy (MRS) can play a role in monitoring early tumour response with examples of preclinical studies and selected clinical studies in tumours of children and young adults. An early non-invasive indicator of tumour response to therapy would provide useful information regarding the effectiveness of therapy. This might be a relevant prognostic factor in new patients and in phase II studies could facilitate recommendations at an early stage as to whether to continue treatment. This review suggests that several markers and ratios are emerging as potential prognostic markers, but larger prospective studies are needed before translating this into clinical practice.

Keywords: MRS; Childhood cancers; Tumour response

1. Introduction

X-rays, ultrasonography, computerised tomography and magnetic resonance imaging (MRI), are conventionally used to evaluate response in solid tumours. With these tools, tumour anatomy, site and size are obtained. Decreasing volume of tumour is generally documented as a sign of response. It may be difficult to ascertain whether the tumour is composed of viable or dead cells and volume change may not occur very rapidly during therapy. Absence of volume response may present assessment difficulties in new cytostatic therapies targeted for example at proliferation or cell cycle control. An early non-invasive indicator of tumour response to therapy would therefore provide useful information regarding the effectiveness of therapy. This might be a relevant prognostic factor in new patients and in phase II studies could facilitate recommendations at an early stage as to whether to continue treatment. This brief review considers to what extent Magnetic Resonance Spectroscopy (MRS) can play a role with examples of pre-clinical studies and selected clinical studies with particular reference to tumours of children and young adults.

MRS is a non-invasive technique, which can be performed using a conventional MRI machine with additional hardware tuned for the frequency of the chosen nucleus, e.g. ^{1}H, ^{13}C, ^{14}N, ^{19}F, ^{23}Na and ^{31}P. The method detects signals from molecules containing the nuclei of interest. The frequency of the signal is dependent on the chemical environment of the nucleus, enabling the different molecules to be distinguished. These frequencies are often displayed as parts per million (ppm) relative to the central frequency. Examples are shown in Figs. 1 and 2. MRS has been widely used to study tumour metabolism.

The initial development of spectroscopy was separate to that of imaging, with early *in vivo* spectrometers having no imaging capabilities. This was rapidly seen to be a drawback for tumour studies, where patient localisation and the morphological data provided by the MR imaging was essential. Most localisation strategies use imaging techniques and modern equipment allows imaging and spectroscopy studies to be integrated. As imaging speed and techniques have improved, it has become possible to combine imaging and spectroscopic studies, providing

* Corresponding author. Tel.: +44-20-8661-3957; fax: +44-20-8661-3617.
E-mail address: rossp@icr.ac.uk (C.R. Pinkerton).

0959-8049/03/$ - see front matter
PII: S0959-8049(02)00728-1

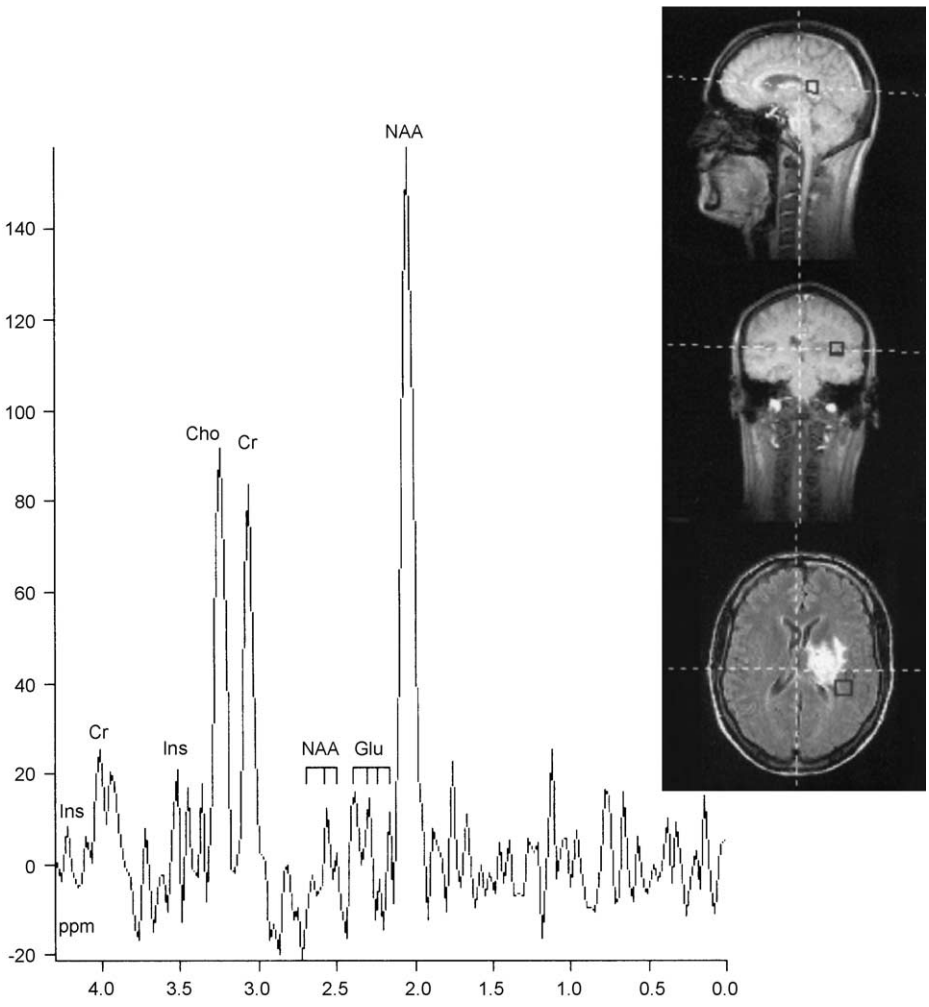

Fig. 1. ^{1}H magnetic resonance spectrum (MRS) of a high-grade glioma showing the various peaks. NAA, *N*-acetyl aspartate; Cr, creatine; Cho, choline, Glu, glutamine and glutamate, Ins, inositol; ppm, parts per million.

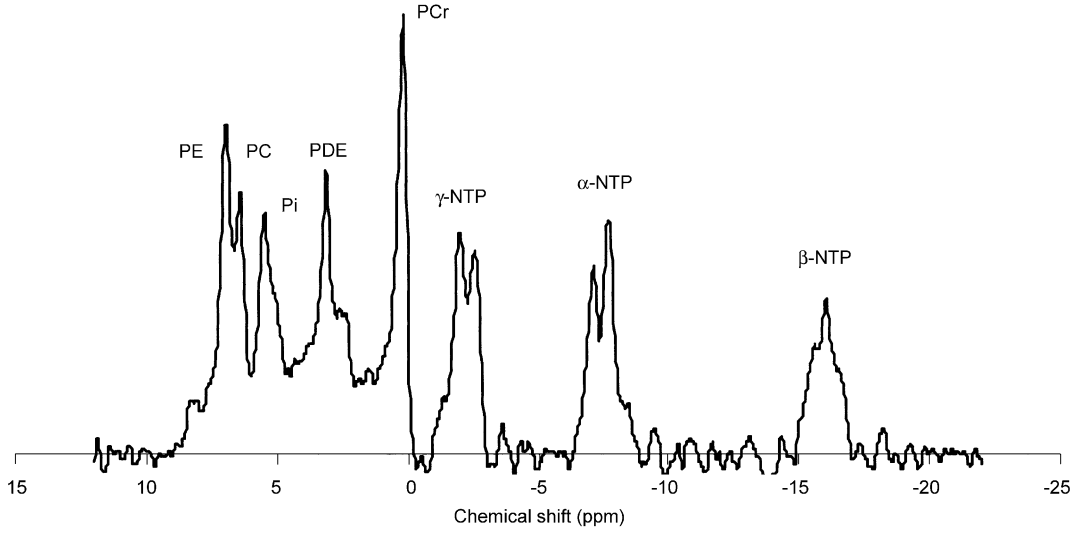

Fig. 2. ^{31}P MRS spectrum of a gastrointestinal stromal tumour. The measurement was performed using 1H-decoupled Chemical Shift Imaging (CSI) with a voxel size of 5×5×5 cm at 1.5T. The tumour shows the various peaks. PE, phosphoethanolamine; PC, phosphocholine; Pi, inorganic phosphate; PDE, phosphodiesters; PCr. phosphocreatine; NTP, nucleoside triphosphate.

complementary imaging, physiological and metabolic information. This remains challenging, but the benefits of integrating such information are showing promise. In a typical MRS exam, MRI images are first acquired for identification of tumour location. Without moving the subject, a process called shimming is then performed to optimise the uniformity of the magnetic field, followed by acquisition of the spectral data. A range of strategies exists for localisation of MRS signals to the region of interest (ROI). Single-voxel methods make use of the intersection of three (usually orthogonal) slices to localise a cuboid. The position of this is specified on the MRI images previously acquired in the same session. The most popular single voxel methods are STEAM (Stimulated Echo Acquisition Mode) [1,2] and PRESS (Point Resolved Spectroscopy) [3] for ^{1}H studies and ISIS (Image Selected In vivo Spectroscopy) [4] for ^{31}P studies. In contrast, socalled Chemical Shift Imaging (CSI) [5], also known as Spectroscopic Imaging, acquires signals from a matrix of voxels, either within a selected slice (2d-CSI) or in three dimensions (3d-CSI) [6]. Such measurements have the advantages of better coverage and potential for the investigation of tissue heterogeneity and, apart from selection of the slice where used, the voxel position can be moved around within the data set after acquisition. Independent phase encoding is required in each spatial dimension so that even a low-resolution 8×8×8 3d matrix requires the acquisition of a minimum of 512 phase encoding steps (taking 8.5 min if a repetition time of 1 s is used). However, each phase-encoding step contributes to the signal of each voxel, so that to a first approximation both types of methods are equally efficient in terms of signal-to-noise ratio (SNR) for a given voxel per unit time. Other factors also affect the relative SNR, such as relaxation times (T1 and T2), point-spread-function and slice profile effects [7].

^{1}H MRS (often referred to as 'proton' MRS) and ^{31}P MRS have been evaluated in cell lines, xenografts and clinical studies. ^{1}H MRS can quantify the relative concentrations of several ^{1}H-containing metabolites from specified tissue regions (Fig. 1). This normally requires suppression of the much larger signals from water and lipids although when adequately localised, lipid signals may also provide valuable information. The principal metabolite signals that can be measured by ^{1}H MRS are *N*-acetyl aspartate (NAA) (in the central nervous system (CNS)), creatine and phosphocreatine (Cr) and choline-containing compounds (Cho). Signals from a range of saturated and unsaturated lipids can also be measured. NAA is present in normal functioning neurons and its signal can be used as a neuronal marker. Creatine and phosphocreatine are important in energy metabolism and levels are constant in normal brain tissue. Creatine is often absent from tumours. Choline-containing compounds are involved in the synthesis and metabolism of cell membranes. Tumours often exhibit high levels of choline compared with normal tissues. Lactate, a marker of anaerobic metabolism, is not usually detected in normal brain, but may be present in brain tumours or areas of ischaemic injury. The presence of lipid in tumours may indicate a higher grade. Several other metabolites such as inositol, myoinositol, glutamate, glutamine, acetate, alanine have also been characterised.

With ^{31}P MRS, signals can be seen from low energy phosphates, i.e. phosphomonoesters (PMEs), inorganic phosphate (Pi), phosphodiesters (PDEs), and from high-energy phosphates i.e. phosphocreatine (PCr) and nucleoside triphosphate (NTP; γ, α and β) (Fig. 2). In comparison with healthy tissues, ^{31}P MR spectra of experimental and clinical tumours generally exhibit elevated PME and PDE signals. The PME signal primarily arises from phospholipid (PL) precursors and PDE arises from phospholipid catabolites and/or mobile phospholipid headgroups. The largest contributions to PME signals arise from phosphocholine (PC) and phosphoethanolamine (PE), which are precursors of the most abundant phospholipid classes in eukaryotic cells, phosphotidylcholine and phosphotidylethanolamine. Phosphomonoesters, such as sugar phosphates and 2,3-diphosphoglycerate, only provide minor contributions to the PME resonance band in tumours, although they are more important in liver. If the magnetic field is homogeneous and if ^{1}H decoupling is used, PME can be further resolved into PE and PC [8,9]. PME levels are interesting spectral and biochemical parameters, in view of their possible role as 'fingerprints' of altered phospholipid turnover and cell proliferation in tumour cells. An increase in PME has been associated with rapid tissue growth or rapid membrane synthesis. PDEs include glycerophosphocholine (GPC) and glycerophospholethanolamine (GPE) and are produced by membrane catabolism. GPC levels may undergo significant reduction during cell maturation, suggesting that this metabolite may be a marker for cell differentiation. While elevated sizes of PC and PE pools may simply reflect high rates of cell proliferation (for either tumour or normal cells), the role of more specific indicators of malignancy might be attributed to spectral parameters such as PC/GPC and PE/PC ratios [10]. High-energy phosphates such as NTP tend to decrease as tumours increase in size, probably because of increased hypoxia. However, due to difficulty in quantitative analysis of peak areas, the MRS data are generally expressed as ratios of metabolites [11].

Magnetic resonance techniques could be applied to image tumour physiology [12,13]. One parameter, which could potentially influence cancer therapeutics, is pH. MRS offers the unique possibility of measuring intracellular and extracellular pH non-invasively, based upon pH dependent changes in the chemical shift of some compounds. Endogenous metabolites with this

property include Pi, the chemical shift of which, when compared with that of PCr or α NTP, gives a measure of pH. Since PCr (often absent in tumours) and NTP are exclusively intracellular and much of the Pi signal comes from the intracellular compartment, this method measures intracellular pH. The extracellular pH can be measured by introducing an exogenous probe. Intracellular pH is tightly controlled and maintained at neutral or slightly alkaline levels, whereas the extracellular pH in tumours is often acidic. The pH gradient across the tumour cell plasma membrane is the reverse of that found in normal tissues. This pH gradient could have implications for cancer therapy and the uptake of drugs [14]. MRS could also play a role in evaluating specific cellular pathways following targeted therapies [15].

In some cases, it is also possible to use MRS to look directly at drugs *in vivo*. Examples include measurement of 5-fluorouracil with ^{19}F MRS and of ifosfamide with ^{31}P MRS [16,17].

MRS is being evaluated as a tool to differentiate benign from malignant lesions, to predict prognosis at diagnosis, to differentiate between scar tissue and active tumour and to monitor the response to therapy.

2. Examples of preclinical studies

The first *in vivo* ^{31}P MRS experiment in an animal tumour model was performed in 1981 [18]. Since then, there have been many studies both in cell lines and xenograft models to evaluate the energy status of tumours [19–21]. Preclinical data have suggested that ^{31}P MRS could be used to provide markers for cell growth, cell kill, response to therapy and to determine resistance to treatment [21,22]. PMEs have been suggested as markers for cellular proliferation and sensitive markers of both tumour regression and regrowth [23].

One example of this type of study investigated the effect of cyclophosphamide on the metabolic profile of implanted mammary carcinoma using ^{31}P MRS both *in vivo* and in perchloric acid extracts [20]. PE/PC ratio increased rapidly during the first 48 h after treatment reflecting a decrease in the PC component. This effect was qualitatively similar to that previously observed following radiation treatment [24]. It appears that the PE/PC ratio is a good indicator of response to both radiation and chemotherapeutic drugs and is a marker of cell kill or cessation of cellular proliferation.

In another study, changes in phosphorus metabolism in a xenografted pharyngeal carcinoma that was sensitive to cisplatin were compared with those occurring in two tumour sub-lines characterised by moderate to high resistance to cisplatin. Prior to cisplatin therapy, no difference in phosphorus metabolism was noted between cell lines, but after cisplatin, alterations in the tumour spectra were related to the degree of tumour response. The earliest and most sensitive marker of tumour regression was a decrease in the phosphomonoester/phosphodiester ratio, paralleled by a gradual increase in phosphocreatine/inorganic phosphate ratio. This suggested that changes detected by ^{31}P MRS following chemotherapy with cisplatin are response specific [21].

Response of xenografted human pharyngeal carcinoma to radiation has also been studied [19]. Alterations in phosphorus metabolism were correlated with growth delay, histological appearance and mitotic activity of the treated tumour. Within 48 h of 30 Gy radiation, there was an increase in the phosphodiester levels, tumour pH and a decrease in phosphomonoester levels. These changes preceded measurable tumour response and were accompanied by extensive histological changes and marked depression of mitotic indices. Pretreatment levels of tumour phospholipids were found to be indicative of radiosensitivity.

Changes in phosphate metabolism have also been used to study tumour growth rate. Normal growth of bladder carcinoma was associated with an increase of inorganic phosphate and phosphomonoesters and a decrease of phosphocreatine [22]. Rapidly growing tumours and early stage of re-growth after treatment with cisplatin showed a high phosphocreatine/beta NTP ratio.

3. Examples of clinical studies

Many studies using ^{31}P MRS show that human cancers, with the exception of glioma, have typical metabolic characteristics that include prominent PME and PDE, low PCr and a pH slightly more alkaline than that of normal cells [25]. Ideally one would like to compare cancer spectra with those of cells which are the normal counterparts from which the cancer arises, but this is only possible in a very few tumour types. Some examples of studies in sarcoma, lymphoma, neuroblastoma and glioma are considered below and summarised in Table 1.

3.1. Soft-tissue sarcoma

The potential prognostic significance of ^{31}P MRS has been studied in sarcomas of the extremity [26]. The aim was to determine whether pretreatment spectra might be useful in defining good risk versus poor risk or predicting responsive versus resistant tumours and to determine whether subsequent changes that occur early during the course of chemotherapy can be used as a predictor of tumour response. 22 patients with suspected soft-tissue sarcoma were studied prior to any treatment. 6 patients subsequently received chemotherapy. The pretreatment spectra of the 3 chemotherapy responsive sarcoma patients were characterised by a relatively lower PDE/PME ratio compared with the

Table 1
Summary of clinical experiments

Ref	Diagnosis	No. patients	Observations
[26]	Soft-tissue sarcoma	22	Pretreatment: Lower PDE/PME ratio in responders During chemotherapy: ↑PDE/PME in responders
[27]	Musculo-skeletal tumour	28	↓ PDE, ↓ PDE/NTP, ↓ PDE/PCr, ↓PDE/Pi in responders
[28]	Musculo-skeletal tumour	28	Pre-treatment: PCr+ Pi/ total phosphate $\geqslant$0.35, PCr/αNTP $\geqslant$1.5, rapid initial ↑ in (PME+ PDE)/(PCr+Pi+NTP) and long-term decrease in responders. In non-responders: PME, Pi and PDE↑
[29]	Neuroblastoma	2	↑PME/β-NTP in progression
[36]	NHL	8	Relative ↑ in Pi peak, ↑PDE, ↓β ATP in responders
[46]	CNS	27	In recurrent tumours, Cho:NAA ratio $\leqslant$4.5—better survival
[47]	CNS (glioma)	10	Tumour Cho/Brain Cho increased with progression
[49]	CNS	10	Pretreatment NAA/Cho, Cr/Cho high in survivors

NHL, non-Hodgkin's lymphoma; CNS, central nervous system; ATP, adenosine triphosphate; PDE, phosphodiester; PME, phosphomonoester; NTP, nucleoside triphosphate; PCr, phosphocreatine; Pi, inorganic phosphate; Cho, choline; NAA, *N*-acetyl aspartate.

spectra of the three non-responsive tumours. Response was defined on the basis of pathological examination and tumour volume. Response was also associated with a large increase in the PDE/PME ratio during the initial cycle of chemotherapy. In contrast, a decrease or minimal increase was noted in two of the three non-responding tumours and an oscillating pattern was seen in the third.

In another study, 28 patients with musculoskeletal tumours were studied with MRS [27]. Elevated levels of PME and PDE were observed relative to normal muscle. There was some overlap between spectral characteristics of different tumour histologies and no association was observed with tumour extent or grade. 15 patients had postchemotherapy MRS, of which 11 showed a reduction in PME, and increase in Pi. 8 patients had surgery. The postchemotherapy MRS was compared with histology. Postchemotherapy reductions in PDE levels of $>20\%$ were associated with a high level of necrosis ($>90\%$) at surgery. An increase in PDE level was associated with a poor histological response. Both PME and PDE are low in muscle tissues and hence possible contamination by adjacent/overlying muscle tissue would have a negligible effect.

In a similar patient group (aged 9–75 years), ^{31}P MRS spectroscopy was studied before starting chemotherapy (32 cases) and serially thereafter during the preoperative chemotherapy [28]. The spectroscopic features were correlated with the percentage of tumour necrosis after surgical resection in 28 patients. Tumours with less than 10% viable cells on histology were defined as responders. By these criteria, 10 were responders. 21 cases were treated on a cooperative study protocol, of which 8 were responders. In the non-responders, PME, Pi and PDE increased whereas energy rich phosphates decreased. In two out of eight responders, the energy-rich phosphates increased whereas others showed features of initial increase in Pi and decrease in PCr followed by increase in high-energy phosphates (biphasic pattern).

3.2. Neuroblastoma

In an innovative study in 1985, two children with neuroblastoma were investigated. Spectral characteristics of an infant with stage IV-S disease were compared with an infant with stage IV disease [29]. NMR spectra from the liver regions in both the infants and primary tumour in the infant with stage IV disease showed substantially elevated PME/β-NTP ratios compared with a spectrum from a normal control. Secondly, ^{31}P NMR spectra from the rapidly enlarging liver (stage IV) and the spontaneously regressing liver (stage IV-S) were quantitatively different. Finally, the ^{31}P NMR spectrum of neuroblastoma changed as a function of time and these changes correlated with clinical observations. The PME/β-NTP ratio increased during periods of rapid progression and persisted until treatment became effective. In this study, however, no field localisation techniques were used and the observed spectra had contributions from the overlying tissue.

3.3. Non-Hodgkin's lymphoma (NHL)

A large prospective multicentre National Cancer Institute funded study is currently documenting treatment-related changes in ^{31}P MRS spectra of adult NHL [30–32]. Spectral changes have been previously described during and after therapy in NHL patients [33–35]. For example, treatment response was studied in 8 newly diagnosed NHL patients using image-guided ^{31}P MRS [36]. Pretreatment spectral characteristics were different in high and low grade NHL. High-grade tumours had a larger Pi peak relative to PME or β-NTP. The PME/Pi ratio produced the best separation between low- and high-grade lymphomas. All patients had serial studies performed after commencing treatment. Changes in tumour metabolites were seen prior to reductions in tumour size. In low-grade lymphomas treated with oral alkylating agents, changes consisted of a relative

increase in Pi peak area and decreased β-NTP followed by increase in the phosphodiesters. This was detected between days 10 and 27 of commencing treatment. For patients with high grade NHL, metabolic changes were detected much earlier (day 3).

^{31}P MRS spectra have also been studied in sera of 35 NHL patients and compared with that of healthy volunteers [37]. In patients with non-responding tumours, the intensities of phospholipid peaks remained relatively low or reduced as the disease progressed, whereas during therapy leading to remission, phospholipids increased resulting in spectra similar to that seen in normal sera.

3.4. Central nervous system (CNS) tumours

By using currently available techniques, ^{31}P MRS of brain tumours does not contribute to the differentiation between different histological types and no correlation to biological malignancy is seen. However, ^{1}H MRS has been extensively used to study brain tumours. The *N*-acetyl aspartate (NAA) signal is reduced in areas of the tumour compared with normal cerebral hemispheres [38]. A co-operative *in vivo* study carried out in 15 clinical research centres confirmed that the 'Cho' resonance was higher in glial tumours than in non-involved brain tissues [39]. Attempts have been made to predict histology and grade and to differentiate tumour from scar tissue or radiation necrosis as well as to evaluate response [40–45].

For example, a study of 27 children with recurrent brain tumours demonstrated the prognostic significance of Cho/NAA ratio in tumour [46]. Diagnoses included high-grade glioma [10], brain stem glioma [7], medulloblastoma/peripheral neuroectodermal tumour [6], ependymoma [3] and pineal germinoma [1]. The concentrations of Cho and NAA in the tumour and normal brain were quantified and maximum Cho/NAA ratio was determined for each patient's tumour. The maximum Cho/NAA ratio ranged from 1.1 to 13.2 (median 4.5). The ratio in apparently normal brain tissue was less than 1. Children with maximum Cho/NAA ratio of less than or equal to 4.5 had a projected survival of more than 50% at 63 weeks and those with ratio of greater than 4.5 had a median survival of 22 weeks, and all 13 children were dead by 63 weeks.

The role of ^{1}H MRS in monitoring response of histologically proven glioma to adjuvant chemotherapy or radiotherapy has also been studied in 10 children [47]. Thirty-eight ^{1}H MRS scans were done. The follow-up period ranged from 6 to 40 months. The ratio of tumour Cho to brain Cho correlated with tumour volume and clinical response. In 4 patients whose tumour progressed after treatment, the tumour choline to brain choline ratio increased and, in 6 patients who had a stable or decreased tumour volume, the ratio decreased.

The resonance profiles of five metabolites measured on ^{1}H MRS imaging spectra (choline-containing compounds, creatine and phosphocreatine, *N*-acetyl groups, lactate and lipids) were studied in 16 adults with recurrent glioma before and during treatment with tamoxifen. MRS imaging metabolite ratios relative to contralateral creatine were studied at 2 weeks and 4 weeks from starting tamoxifen. Responders and the non-responder group differed significantly in the mean intensities of the five metabolites, both at the pretreatment evaluation and 2 weeks evaluation [48].

Peak areas of NAA, Cho, creatine and phosphocreatine were assessed in 14 young people (average 10 years) with newly diagnosed cerebral hemispheric tumours. There were three glioblastomas and one each of primitive neuroectodermal tumours (PNET), ganglio-glioblastoma, ependymoma, anaplastic ependymoma, rhabdoid teratoid tumour, pilocytic astrocytoma and gliomatosis cerebri and four gangliogliomas. 4 patients died and 10 survived. The NAA/Cho and creatine/choline ratios were low in patients who died and high in the survivors [49].

4. Conclusions

Many studies have shown that ^{1}H and ^{31}P MRS measurements detect *in vivo* biochemical changes in normal tissue and tumours following treatment. This has been seen in a range of tumour types. However, there is a lack of consistency in the descriptive measures used. Many studies include a range of histological types that may mask effects specific to each class. In addition, the range of treatments, variability in defining response and different localisation strategies used make interpretation difficult. There is, therefore, a need for standardised methodology to enable comparison between studies and to understand the basis of the changes observed. This could be made possible by conducting large disease-specific multicentre trials with standardised methodology. It is evident from the review of literature that several markers and ratios are emerging as potential prognostic markers of tumour response. For example, a decrease in PME could suggest a responsive tumour and could help to tailor treatment for a patient depending on early response and therefore potentially avoid the use of non-effective therapies. It could play a role in identifying patients who could fail therapy and in these patients second-line treatment could be initiated at an earlier stage. In phase II studies, this could have implications for the early evaluation of efficacy.

Acknowledgements

Professor Pinkerton, Professor Leach and Dr Payne are supported by Cancer Research UK.

References

1. Frahm J, Bruhn H, Gyngell ML, Merboldt KD, Hanicke W, Sauter R. Localized high-resolution proton NMR spectroscopy using stimulated echoes: initial applications to human brain *in vivo*. *Magn Reson Med* 1989, **9**, 79–93.
2. Frahm J, Merboldt KD, Hanicke W. Localized proton spectroscopy using stimulated echoes. *J Magn Reson* 1987, **72**, 502–508.
3. Bottomley PA. Spatial localization in NMR spectroscopy *in vivo*. *Ann NY Acad Sci* 1987, **508**, 333–348.
4. Ordidge R, Connelly A, Lohman J. Image-selected *in vivo* spectroscopy (ISIS). A new technique for spatially selective NMR spectroscopy. *J Magn Reson* 1986, **66**, 283–294.
5. Brown TR, Kincaid BM, Ugurbil K. NMR chemical shift imaging in three dimensions. *Proc Natl Acad Sci USA* 1982, **79**, 3523–3526.
6. Brown TR. Practical applications of chemical shift imaging. *NMR Biomed* 1992, **5**, 238–243.
7. Moonen CT, von Kienlin M, van Zijl PC, *et al*. Comparison of single-shot localization methods (STEAM and PRESS) for *in vivo* proton NMR spectroscopy. *NMR Biomed* 1989, **2**, 201–208.
8. Freeman DM, Hurd R. Decoupling: theory and practice. II. State of the art: *in vivo* applications of decoupling. *NMR Biomed* 1997, **10**, 381–393.
9. Luyten PR, Bruntink G, Sloff FM, *et al*. Broadband proton decoupling in human 31P NMR spectroscopy. *NMR Biomed* 1989, **1**, 177–183.
10. Podo F. Tumour phospholipid metabolism. *NMR Biomed* 1999, **12**, 413–439.
11. Leach MO, Le Moyec L, Podo F. MRS of tumours: basic principles. In de Certaines JD, Bovee W, Podo F, eds. *Magnetic Resonance Spectroscopy in Biology and Medicine*. UK, Pergamon Press, 1992, 295–344.
12. Stubbs M. Application of magnetic resonance techniques for imaging tumour physiology. *Acta Oncol* 1999, **38**, 845–853.
13. Evelhoch JL, Gillies RJ, Karczmar GS, *et al*. Applications of magnetic resonance in model systems: cancer therapeutics. *Neoplasia* 2000, **2**, 152–165.
14. Ojugo AS, McSheehy PM, Stubbs M, *et al*. Influence of pH on the uptake of 5-fluorouracil into isolated tumour cells. *Br J Cancer* 1998, **77**, 873–879.
15. Ronen SM, Jackson LE, Beloueche M, Leach MO. Magnetic resonance detects changes in phosphocholine associated with Ras activation and inhibition in NIH 3T3 cells. *Br J Cancer* 2001, **84**, 691–696.
16. Findlay MP, Leach MO. *In vivo* monitoring of fluoropyrimidine metabolites: magnetic resonance spectroscopy in the evaluation of 5-fluorouracil. *Anticancer Drugs* 1994, **5**, 260–280.
17. Payne GS, Pinkerton CR, Bouffet E, Leach MO. Initial measurements of ifosfamide and cyclophosphamide in patients using ^{31}P MRS: pulse-and-acquire, decoupling, and polarization transfer. *Magn Reson Med* 2000, **44**, 180–184.
18. Griffiths JR, Stevens AN, Iles RA, Gordon RE, Shaw D. 31P-NMR investigation of solid tumours in the living rat. *Biosci Rep* 1981, **1**, 319–325.
19. Jackel MC, Kopf-Maier P, Baumgart F, Ziessow D, Tausch-Treml R. Value of 31P NMR spectroscopy in predicting the response of a xenografted human hypopharynx carcinoma to irradiation. *J Cancer Res Clin Oncol* 2000, **126**, 325–331.
20. Street JC, Mahmood U, Matei C, Koutcher JA. *In vivo* and *in vitro* studies of cyclophosphamide chemotherapy in a mouse mammary carcinoma by 31P NMR spectroscopy. *NMR Biomed* 1995, **8**, 149–158.
21. Tausch-Treml R, Kopf-Maier P, Baumgart F, *et al*. 31P nuclear magnetic resonance spectroscopy, histology and cytokinetics of a xenografted hypopharynx carcinoma following treatment with cisplatin: comparison in three sublines with increasing resistance. *Br J Cancer* 1991, **64**, 485–493.
22. de Certaines JD, Albrectsen J, Larsen VA, Xie X, Rygaard J, Henriksen O. *In vivo* 31P magnetic resonance spectroscopy and 1H magnetic resonance imaging of human bladder carcinoma on nude mice: effects of tumour growth and treatment with cis-dichloro-diamine platinum. *In Vivo* 1992, **6**, 611–616.
23. de Certaines JD, Larsen VA, Podo F, Carpinelli G, Briot O, Henriksen O. *In vivo* 31P MRS of experimental tumours. *NMR Biomed* 1993, **6**, 345–365.
24. Koutcher JA, Alfieri AA, Devitt ML, *et al*. Quantitative changes in tumor metabolism, partial pressure of oxygen, and radiobiological oxygenation status postradiation. *Cancer Res* 1992, **52**, 4620–4627.
25. Negendank W. Studies of human tumors by MRS: a review. *NMR Biomed* 1992, **5**, 303–324.
26. Koutcher JA, Ballon D, Graham M, *et al*. 31P NMR spectra of extremity sarcomas: diversity of metabolic profiles and changes in response to chemotherapy. *Magn Reson Med* 1990, **16**, 19–34.
27. Redmond OM, Bell E, Stack JP, *et al*. Tissue characterization and assessment of preoperative chemotherapeutic response in musculoskeletal tumors by *in vivo* 31P magnetic resonance spectroscopy. *Magn Reson Med* 1992, **27**, 226–237.
28. Moller HE, Vermathen P, Rummeny E, *et al*. *In vivo* 31P NMR spectroscopy of human musculoskeletal tumors as a measure of response to chemotherapy. *NMR Biomed* 1996, **9**, 347–358.
29. Maris JM, Evans AE, McLaughlin AC, *et al*. 31P nuclear magnetic resonance spectroscopic investigation of human neuroblastoma *in situ*. *N Engl J Med* 1985, **312**, 1500–1505.
30. Arias-Mendoza F, Brown, TR, Charles HC, *et al*. Methodological standardization for a multi-institutional *in vivo* trial of localized 31P MR spectroscopy in human cancer research. In *Proceedings of the 7th Annual Meeting of the International Society of Magnetic Resonance in Medicine*, 1999, 1585 (abstr).
31. Arias-Mendoza F, Brown TR, Schwartz AJ, *et al*. Preliminary results of a multi-instituitional trial to demonstrate clinical predictive value of *in vivo* localized 31P MR spectroscopy data in human non-Hodgkin's lymphoma. In *Proceedings of the 8th Annual Meeting of the International Society of Magnetic Resonance in Medicine*, 2000, 98 (abstr).
32. Arias-Mendoza F, Zakian K, Stubbs M, *et al*. Investigation of the predictive value of the pretreatment tumour content of phosphoethanolamine and phosphocholine measured by *in vivo* 31P MR spectroscopy in non-Hodgkin's lymphoma in a multi-instituitional setting. In *Proceedings of the 9th Annual Meeting of the International Society of MAgnetic Resonance in Medicine*, 2001, 274 (abstr).
33. Bizzi A, Movsas B, Tedeschi G, *et al*. Response of non-Hodgkin lymphoma to radiation therapy: early and long-term assessment with H-1 MR spectroscopic imaging. *Radiology* 1995, **194**, 271–276.
34. Bryant DJ, Bydder GM, Case HA, *et al*. Use of phosphorus-31 MR spectroscopy to monitor response to chemotherapy in non-Hodgkin lymphoma. *J Comput Assist Tomogr* 1988, **12**, 770–774.
35. Negendank WG, Padavic-Shaller KA, Li CW, *et al*. Metabolic characterization of human non-Hodgkin's lymphomas *in vivo* with the use of proton-decoupled phosphorus magnetic resonance spectroscopy. *Cancer Res* 1995, **55**, 3286–3294.
36. Smith SR, Martin PA, Davies JM, Edwards RH, Stevens AN. The assessment of treatment response in non-Hodgkin's lymphoma by image guided 31P magnetic resonance spectroscopy. *Br J Cancer* 1990, **61**, 485–490.
37. Kuliszkiewicz-Janus M, Baczynski S. Application of 31P NMR spectroscopy to monitor chemotherapy-associated changes of serum phospholipids in patients with malignant lymphomas. *Magn Reson Med* 1996, **35**, 449–456.
38. Heesters MA, Kamman RL, Mooyaart EL, Go KG. Localized

proton spectroscopy of inoperable brain gliomas. Response to radiation therapy. *J Neurooncol* 1993, **17**, 27–35.
39. Negendank WG, Sauter R, Brown TR, *et al*. Proton magnetic resonance spectroscopy in patients with glial tumors: a multicenter study. *J Neurosurg* 1996, **84**, 449–458.
40. Wang Z, Sutton LN, Cnaan A, *et al*. Proton MR spectroscopy of pediatric cerebellar tumors. *AJNR Am J Neuroradiol* 1995, **16**, 1821–1833.
41. Tedeschi G, Lundbom N, Raman R, *et al*. Increased choline signal coinciding with malignant degeneration of cerebral gliomas: a serial proton magnetic resonance spectroscopy imaging study. *J Neurosurg* 1997, **87**, 516–524.
42. Taylor JS, Langston JW, Reddick WE, *et al*. Clinical value of proton magnetic resonance spectroscopy for differentiating recurrent or residual brain tumor from delayed cerebral necrosis. *Int J Radiat Oncol Biol Phys* 1996, **36**, 1251–1261.
43. Hwang JH, Egnaczyk GF, Ballard E, Dunn RS, Holland SK, Ball Jr WS. Proton MR spectroscopic characteristics of pediatric pilocytic astrocytomas. *AJNR Am J Neuroradiol* 1998, **19**, 535–540.
44. Lin A, Bluml S, Mamelak AN. Efficacy of proton magnetic resonance spectroscopy in clinical decision making for patients with suspected malignant brain tumors. *J Neurooncol* 1999, **45**, 69–81.
45. Preul MC, Caramanos Z, Collins DL, *et al*. Accurate, noninvasive diagnosis of human brain tumors by using proton magnetic resonance spectroscopy. *Nat Med* 1996, **2**, 323–325.
46. Warren KE, Frank JA, Black JL, *et al*. Proton magnetic resonance spectroscopic imaging in children with recurrent primary brain tumors. *J Clin Oncol* 2000, **18**, 1020–1026.
47. Lazareff JA, Gupta RK, Alger J. Variation of post-treatment H-MRSI choline intensity in pediatric gliomas. *J Neurooncol* 1999, **41**, 291–298.
48. Preul MC, Caramanos Z, Villemure JG, *et al*. Using proton magnetic resonance spectroscopic imaging to predict *in vivo* the response of recurrent malignant gliomas to tamoxifen chemotherapy. *Neurosurgery* 2000, **46**, 306–318.
49. Girard N, Wang ZJ, Erbetta A, *et al*. Prognostic value of proton MR spectroscopy of cerebral hemisphere tumors in children. *Neuroradiology* 1998, **40**, 121–125.